

---

# PARTIAL INVERSE DESIGN OF HIGH-PERFORMANCE CONCRETE USING COOPERATIVE NEURAL NETWORKS FOR CONSTRAINT-AWARE MIX GENERATION

---

**Agung Nugraha**

Department of Industrial and Data Engineering  
Pukyong National University  
Republic of Korea  
agung@pukyong.ac.kr

**Heungjun Im**

Department of Industrial and Data Engineering  
Pukyong National University  
Republic of Korea  
heungjun37@pukyong.ac.kr

**Jihwan Lee** \*

Department of Industrial and Data Engineering  
Pukyong National University  
Republic of Korea  
jihwan@pknu.ac.kr

## ABSTRACT

High-performance concrete requires complex mix design decisions involving interdependent variables and practical constraints. While data-driven methods have improved predictive modeling for forward design in concrete engineering, inverse design remains limited, especially when some variables are fixed and only the remaining ones must be inferred. This study proposes a cooperative neural network framework for the partial inverse design of high-performance concrete. The framework integrates an imputation model with a surrogate strength predictor and learns through cooperative training. Once trained, it generates valid and performance-consistent mix designs in a single forward pass without retraining for different constraint scenarios. Compared with baseline models, including autoencoder models and Bayesian inference with Gaussian process surrogates, the proposed method achieves R-squared values of 0.87 to 0.92 and substantially reduces mean squared error by approximately 50% and 70%, respectively. The results show that the framework provides an accurate and computationally efficient foundation for constraint-aware, data-driven mix proportioning.

**Keywords** High-performance concrete · Data-driven design · Partial inverse design · Surrogate model · Imputation model · Autoencoder

## 1 Introduction

High-performance concrete (HPC) is an advanced construction material valued for its superior strength and durability. Unlike conventional concrete, which primarily consists of Portland cement, fine and coarse aggregates, and water, HPC incorporates supplementary cementitious materials (SCMs) such as fly ash and blast furnace slag, together with chemical admixtures such as superplasticizers [1, 2]. These blended cement systems enhance workability, improve long-term performance, and reduce the environmental impact by lowering the dependence on Portland cement, which is a significant contributor to CO<sub>2</sub> emissions. As a result, HPC supports both structural efficiency and environmental sustainability in construction [1, 3].

Alongside material innovations and the increasing availability of high-quality experimental data, the data-driven design (DDD) paradigm has emerged as a transformative approach in concrete research and materials science [4, 5, 6, 7]. DDD is broadly defined as a methodology in which empirical or simulated data serve as the foundation for predictive or

---

\*Corresponding author's

generative modeling to support engineering decision-making [8, 9]. Unlike conventional approaches that rely heavily on explicit physical or mechanistic models, DDD employs predictive models that capture the complex and often nonlinear relationships directly from data. In doing so, it enables rapid property prediction, reduces the need for time-consuming experiments or costly simulations, and facilitates the intelligent exploration of complex design spaces.

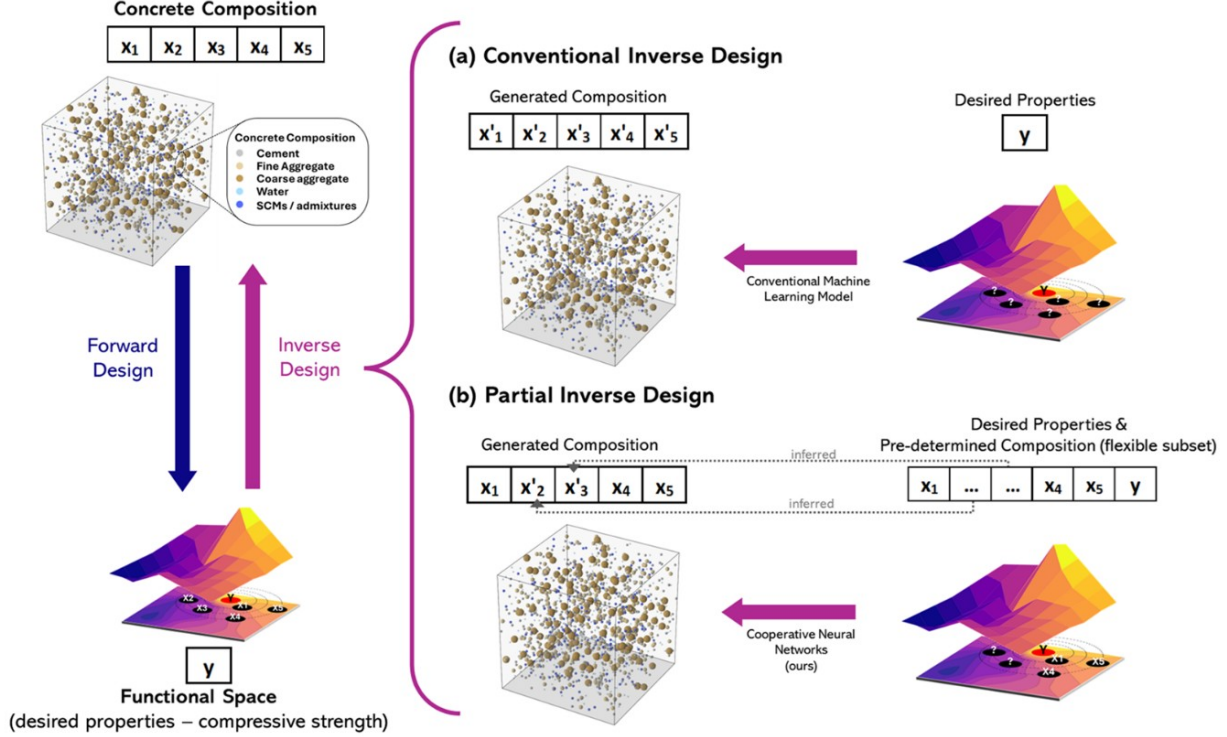


Figure 1: The DDD paradigm of forward design, inverse design and partial inverse design.

Within the data-driven design paradigm, design tasks can be categorized into distinct approaches. Forward design (as illustrated in Fig. 1) represents the predictive approach, in which known input variables (e.g., mix proportions) are used to estimate material properties such as compressive strength. This process involves developing a predictive or surrogate model that serves as an efficient substitute for complex and computationally expensive physical models [10, 11]. The surrogate model learns from available data on design parameters and their corresponding performance metrics, enabling rapid and reliable evaluation of candidate mix design solutions. One of the early applications of machine learning-based surrogate modeling in the concrete domain was introduced by Yeh in 1998 [2], who developed an artificial neural network (ANN) model to predict compressive strength of HPC. The study concluded that ANN outperformed traditional regression models in accuracy and proved to be a convenient tool for analyzing the effects of mix proportion variables through numerical experiments. Following this methodology, Yeh in 2006 [12] also applied neural networks as surrogate models in combination with design of experiments to investigate the effects of fly ash replacement, curing age, and water-binder ratio on the compressive strength of both low- and high-strength concrete. Later on, with the rapid advancement of machine learning research, various algorithms were applied in the cement and concrete domain [13], including ANN [14, 15, 16, 17, 18], polynomial neural network hybrid models [4], support vector machine (SVM) and its hybrid model [16, 18, 19], Gaussian process (GP) model [1, 20], decision tree-based model [20, 21], ensemble model [5, 15, 16, 18, 20, 21, 22, 23], and other combination or hybrid approaches [24, 25]. Fazel Zarandi et al. in 2008 [4] constructed and evaluated six hybrid neural network frameworks integrating fuzzy logic with polynomial neural networks, aiming to identify the most effective model for predicting the compressive strength of concrete mix designs. Cheng et al. in 2012 [19] developed a hybrid model that integrated Fuzzy Logic (FL), weighted SVM, and fast messy genetic algorithm (fmGA) into an adaptive system called Evolutionary Fuzzy Support Vector Machine Inference Model for Time Series Data (EFSIMT), demonstrating its effectiveness in predicting the compressive strength of concrete. Ke and Duan in 2021 [1] employed GP models as surrogate models in their inverse design architecture to predict concrete compressive strength, highlighting their ease of integration with Bayesian

inference methods. More recently, the application of surrogate models to predict compressive strength in advanced concretes has been demonstrated by several studies. Wijesundara et al. in 2025 [5] evaluated seven predictive models, including SVM, ensemble tree models, and multi-layer perceptron (MLP), for ultra-high-performance fiber-reinforced concrete (UHPFRC). M. Ishana et al. in 2025 [25] developed a hybrid model that combines ANN with a genetic algorithm (GA), referred to as ANN-GA, for HPC.

In contrast, inverse design represents a target-driven paradigm that reverses the usual direction of prediction. Rather than estimating material properties from known mix compositions, it determines the combination of design variables required to achieve a specified target property, such as compressive strength (Fig. 1). Conceptually, it seeks to map desired outcomes back to feasible material configurations, a process often referred to as design inversion in materials informatics. In data-driven contexts, inverse design architectures are generally realized in two forms: (a) single-stage approaches, where the configurations are determined directly using models such as generative neural networks, and (b) two-stage approaches, where surrogate models are integrated with complementary mechanisms to refine or guide the generation of valid designs [26]. In concrete research, these mechanisms have led to several methodological approaches, including optimization-based, Bayesian and probabilistic inference, and generative approaches, each differing in how the inversion process is formulated.

The most established class in concrete research comprises optimization-based approaches, where a surrogate predictive model is first trained to approximate the relationship between design variables and material properties, and then combined with a search-based method or an optimization algorithm to iteratively identify compositions satisfying the target performance. Huang et al. in 2020 [27] developed an inverse design framework that coupled SVR with a Firefly Algorithm to optimize mixture proportions for steel fiber-reinforced concrete (SFRC). Similarly, Zhang et al. in 2020 [28] proposed a hybrid intelligent system that integrates multiple AI-based surrogate models with a metaheuristic optimizer to design recycled aggregate concrete satisfying multiple objectives. Recently, Le Nguyen et al. in 2024 [29] employed several predictive tree-based machine learning models coupled with a Fast Elitist Non-Dominated Sorting Genetic Algorithm for Multi-Objective Optimization (NSGA-II) to iteratively evolve optimal concrete mix proportions. Utilizing similar machine learning model, Zhang et al. in 2025 [30] introduced a Bayesian Optimization XGBoost (BO-XGBoost) framework for lightweight strain-hardening UHPC, where transfer learning was applied to the XGBoost surrogate to enhance generalization under data scarcity. These surrogate-guided optimization methods enable interpretable and flexible design exploration but can be computationally intensive due to their iterative nature.

Beyond optimization-based frameworks, other approaches have emerged that tackle the inverse problem from different perspectives. Bayesian and probabilistic inference methods treat inverse design as a problem of posterior estimation rather than optimization, inferring a distribution of feasible inputs that satisfy a target property and thereby capturing uncertainty in the design space. Ke and Duan in 2021 [1] exemplified this paradigm by combining a GP surrogate with the Metropolis–Hastings (MH) algorithm in a Markov Chain Monte Carlo (MCMC) framework, enabling probabilistic inference of high-performance concrete compositions that achieve desired compressive strengths. In parallel, direct-generation approaches based on generative or encoder-decoder neural networks have gained attention for learning the inverse mapping explicitly, thereby eliminating the need for iterative search. Once trained, these models can generate candidate mix designs in a single forward pass conditioned on desired performance targets. Yu et al. in 2023 [31], for example, developed a generative AI framework for the performance-based design of engineered cementitious composites (ECC), employing an invertible neural network (INN) to directly generate mix proportions that satisfy target tensile strength and strain requirements. While Bayesian approaches emphasize probabilistic reasoning and uncertainty estimation, direct-generation models focus on efficient one-shot inference. Despite their respective computational and data challenges, both offer promising directions for advancing data-driven inverse design in concrete mix design.

Despite recent advances, existing inverse design studies share a fundamental limitation that they are primarily designed to generate complete mix designs and cannot flexibly handle situations where only part of the composition should be optimized [1, 27, 28, 29, 30, 31]. Most frameworks assume that all design variables are freely adjustable, but in practice, this assumption may not always hold. Concrete mix design in real construction projects is subject to multiple constraints, where certain variables are predetermined by construction standards, cost limits, or material availability. In these cases, designers often need to adjust only a subset of variables while keeping others fixed to satisfy project-specific or regulatory requirements [32]. However, existing inverse design methods cannot selectively infer unknown variables while maintaining fixed ones, making them unsuitable for modular or hierarchical design workflows where partial reconfiguration of a mix is required instead of complete redesign.

This challenge defines the partial inverse design problem, in which only a portion of design variables is unknown and must be estimated under specific constraints. Conceptually, this problem can be formulated as a constrained optimization task [33]. Prior approaches have typically relied on iterative optimization frameworks, such as Bayesian optimization or other search-based methods [34, 35], which are computationally expensive and difficult to generalize to varying constraint conditions.

To address this limitation, this study applies and extends a previously developed Cooperative Neural Network (CoNN) framework [26] to directly perform partial inverse design for HPC. The framework reformulates partial inverse design as a constraint-aware imputation problem, in which missing design variables are reconstructed to meet a specified target property. It integrates two key components, an imputation model based on an autoencoder architecture that reconstructs incomplete mix designs from partially masked inputs, and a surrogate performance predictor that estimates compressive strength from complete designs and provides feedback during cooperative training. During training, the two models interact in a cooperative learning loop, where the imputation model generates candidate designs for missing variables and the surrogate model evaluates their predicted strength to guide reconstruction accuracy. This joint optimization enables the network to produce designs that are both numerically consistent with the training data and physically meaningful with respect to target performance. Unlike iterative optimization methods such as Bayesian optimization, the trained CoNN generates feasible mix compositions in a single forward pass, allowing instant inference without retraining even when constraint conditions change. The framework is evaluated on a benchmark HPC dataset to validate its accuracy, stability, and efficiency under limited-data conditions. The results show that the CoNN achieves higher predictive accuracy and computational efficiency than conventional search-based methods, demonstrating its suitability for data-driven material design tasks where only part of the composition is adjustable.

The remainder of this paper is structured as follows. Section 2 details the methodology, including the components and integration of the cooperative framework for inverse design of HPC. Section 3 outlines the experimental and evaluation setup, including dataset description, preprocessing, inference configurations, evaluation objective, and baseline models for comparison. Section 4 presents the experimental results, highlighting key findings and practical implications. Finally, Section 5 concludes the paper by summarizing the contributions and discussing limitations and directions for future research.

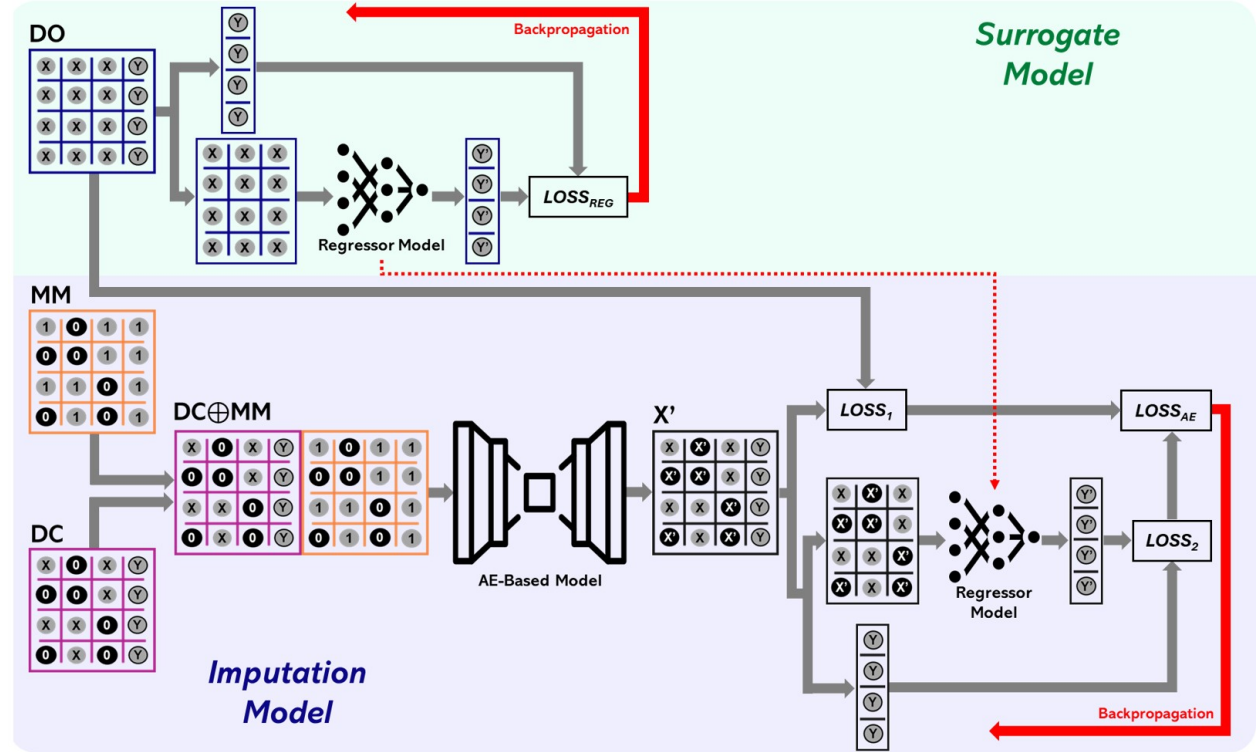


Figure 2: Cooperative Neural Network (CoNN) (adopted from [26]). Schematic illustration of the CoNN framework for partial inverse design of HPC. The upper (green) region shows the surrogate model predicting compressive strength from complete mix designs, while the lower (purple) region shows the autoencoder-based imputation model reconstructing masked variables. CoNN is optimized cooperatively through reconstruction ( $\mathcal{L}_1$ ) and performance ( $\mathcal{L}_2$ ) objectives, combined into a unified loss ( $\mathcal{L}_{AE}$ ). Red arrows indicate the backpropagation flow connecting both models, forming a feedback loop that aligns reconstructed compositions with desired performance targets.

## 2 Cooperative Neural Networks

This study adapts the Cooperative Neural Network (CoNN) framework introduced by Nugraha et al. [26] to the problem of partial inverse design of HPC under multi-constraint conditions. In this context, partial inverse design refers to estimating the unknown portion of a mix composition when some ingredients (e.g., water-binder ratio or supplementary cementitious material contents) are predetermined by engineering constraints or experimental setup, while still satisfying a target compressive strength. The CoNN architecture couples two models, a surrogate model and an imputation model that learn cooperatively to reconstruct feasible mix designs from incomplete inputs.

The framework operates on a dataset  $\mathbf{X} \in \mathbb{R}^{n \times d}$ , where each row corresponds to a concrete batch (either experimentally measured or simulated) and each column represents one design variable such as cement, water, blast-furnace slag (BFS), fly ash (PFA), superplasticizer (SP), fine aggregate (FA), coarse aggregate (CA), and curing age. The corresponding target property  $\mathbf{y} \in \mathbb{R}^n$  denotes the experimentally measured compressive strength (MPa). In practice, this dataset can be obtained from laboratory experiments, field tests, or simulation-based mix-design studies, depending on availability. The overall architecture of the proposed framework is illustrated in Fig. 2.

### 2.1 Surrogate Model

The surrogate model, depicted in the upper part of Fig. 2, approximates the nonlinear mapping between mix composition and compressive strength as  $\hat{\mathbf{y}} = f(\mathbf{X})$ , where  $f(\cdot)$  denotes an ANN regressor. From the original dataset **DO**, the model takes the complete mix-design variables  $\mathbf{X}$  as input and predicts the corresponding compressive strength  $\hat{\mathbf{y}}$ . Training minimizes the mean-squared error between the measured and predicted strengths:

$$\mathcal{L}_{\text{REG}} = \frac{1}{N} \sum_{i=1}^N (y_i - \hat{y}_i)^2 \quad (1)$$

where  $N$  is the number of samples. Minimizing  $\mathcal{L}_{\text{REG}}$  enables the surrogate model to capture the forward relationship between concrete mix proportions and compressive strength. Once trained, it collaborates with the imputation model, providing performance-based feedback that guides the generation of strength-consistent mix designs.

### 2.2 The Imputation Model

The imputation model, shown in the lower part of Fig. 2, is based on an autoencoder (AE) architecture that reconstructs missing mix variables from partially specified data. By learning a compact latent representation, the model infers unknown variables from the available context. Its inputs are:

- **DO**: the original complete mix-design data (including the performance criterion  $\mathbf{y}$ ),
- **DC**: a corrupted version of **DO** obtained by replacing a subset of variables with zeros, and
- **MM**: a binary mask matrix indicating observed (1) and missing (0) variables.

To make the encoder aware of which features are missing, **DC** and **MM** are concatenated column-wise to form the input (**DC**  $\oplus$  **MM**). The encoder  $f(\cdot)$  transforms this combined input into a latent representation.

$$\mathbf{z} = f(\mathbf{DC} \oplus \mathbf{MM}) \quad (2)$$

The decoder  $g(\mathbf{z})$  reconstructs a complete mix design. To ensure that the generated values remain within the empirically valid domain (e.g., unrealistic or physically infeasible mix quantities), feature clipping is applied by constraining each reconstructed variable to the per-feature minimum ( $\mathbf{X}_{\min}$ ) and maximum ( $\mathbf{X}_{\max}$ ) values from the training dataset:

$$\hat{\mathbf{X}} = \min(\max(g(\mathbf{z}), \mathbf{X}_{\min}), \mathbf{X}_{\max}) \quad (3)$$

The reconstructed output is merged with the unmasked components of the input to obtain the completed design parameters

$$\mathbf{X}' = (\mathbf{1} - \mathbf{MM}) \odot \hat{\mathbf{X}} + \mathbf{DC} \quad (4)$$

where  $\odot$  denotes element-wise multiplication.

### 2.3 Cooperative Learning Mechanism

During training, the imputation model generates completed design parameters  $\mathbf{X}'$ , and the surrogate model evaluates their predicted compressive strength as  $\hat{y} = f(\mathbf{X}')$ . Two complementary objectives are optimized jointly: the reconstruction loss ( $\mathcal{L}_1$ ), which measures the difference between the reconstructed and original designs, and the performance loss ( $\mathcal{L}_2$ ), which quantifies the deviation between predicted and measured strengths. These are combined into a unified cooperative loss.

$$\mathcal{L}_{\text{TOTAL}} = \mathcal{L}_{\text{AE}} = \alpha \mathcal{L}_1 + (1 - \alpha) \mathcal{L}_2 \quad (5)$$

where  $\alpha \in [0, 1]$  controls the trade-off between reconstruction fidelity and performance consistency. Through this cooperative feedback, the imputation model learns to generate statistically plausible and performance-compliant compositions. This optimization establishes the core mechanism of the CoNN.

### 2.4 Imputation Model Variants

Depending on the target application, the imputation model can adopt deterministic or generative denoising variants while maintaining the same cooperative structure:

- **Cooperative DAE (Denoising Autoencoder):** a deterministic model minimizing  $\mathcal{L}_{\text{TOTAL}}$ , suited for one-to-one reconstruction of specific HPC mix designs.
- **Cooperative DVAE (Denoising Variational Autoencoder):** introduces a probabilistic latent variable and a Kullback–Leibler divergence term  $D_{\text{KL}}(q(\mathbf{z} \mid \mathbf{X}) \parallel p(\mathbf{z}))$  to capture uncertainty and generate multiple valid design candidates.
- **Cooperative DWAE (Denoising Wasserstein Autoencoder):** replaces the KL divergence with a Maximum Mean Discrepancy (MMD) term  $\text{MMD}_k^2(q(\mathbf{z}), p(\mathbf{z}))$  to enforce smoother latent distributions and improve robustness under limited data.

All variants share the same cooperative loss defined in Eq. 5, each with slight modifications reflecting their respective objective functions, and the same two-model structure shown in Fig. 2. This flexibility allows the framework to support both deterministic optimization and generative exploration, enabling the generation of diverse, performance-consistent mix designs within a unified learning architecture. More details on the VAE variant can be found in the original work by Kingma and Welling [36], and on the WAE variant in the work by Tolstikhin et al. [37].

## 3 Experimental Setup and Evaluation

This section describes the dataset, preprocessing, and experimental configuration used to evaluate the CoNN framework. The setup was designed to ensure a fair and comprehensive assessment of model performance and to provide consistent conditions for comparison with baseline approaches.

Table 1: Dataset information of HPC.

Feature Name	Description (with Units)
Cement	Cement content in the mix (kg/m <sup>3</sup> )
BFS	Blast Furnace Slag content (kg/m <sup>3</sup> )
PFA	Fly Ash content (kg/m <sup>3</sup> )
Water	Amount of water in the mix (kg/m <sup>3</sup> )
SP	Superplasticizer dosage (kg/m <sup>3</sup> )
CA	Coarse Aggregate content (kg/m <sup>3</sup> )
FA	Fine Aggregate content (kg/m <sup>3</sup> )
Age	Concrete curing time (days)
Strength	Compressive strength of concrete (MPa)

### 3.1 Dataset Description

A publicly available concrete dataset originally collected by Yeh [2] was used for all experiments. This dataset has been widely adopted in previous data-driven concrete research and thus provides a reliable benchmark for comparative

studies. It contains 1,030 records of concrete mix ingredients and their corresponding compressive strengths. The variables and their physical units are summarized in Table 1.

To align with the focus on HPC, only samples with curing ages of up to 28 days were retained, as this period captures the majority of strength development in HPC [1, 30, 32]. Furthermore, this restriction was also applied to emphasize early-age strength development, representing the most critical curing period for HPC [3]. After filtering, a total of 749 records out of 1,030 concrete specimens were used in this study.

### 3.2 Data Preprocessing and Splitting

The dataset was divided into training and testing subsets using an 8:2 split ratio, which balanced model learning with unbiased generalization assessment. Because the dataset is relatively small, we repeated the splitting process five times with different random seeds and reported the average performance across these five folds. Each split produced 600 training and 149 testing samples. Fig. 3 confirms that no noticeable distributional bias was introduced by the splitting process. All input variables were normalized so that features measured on different scales contributed comparably during training and no single variable dominated the gradient updates [1].

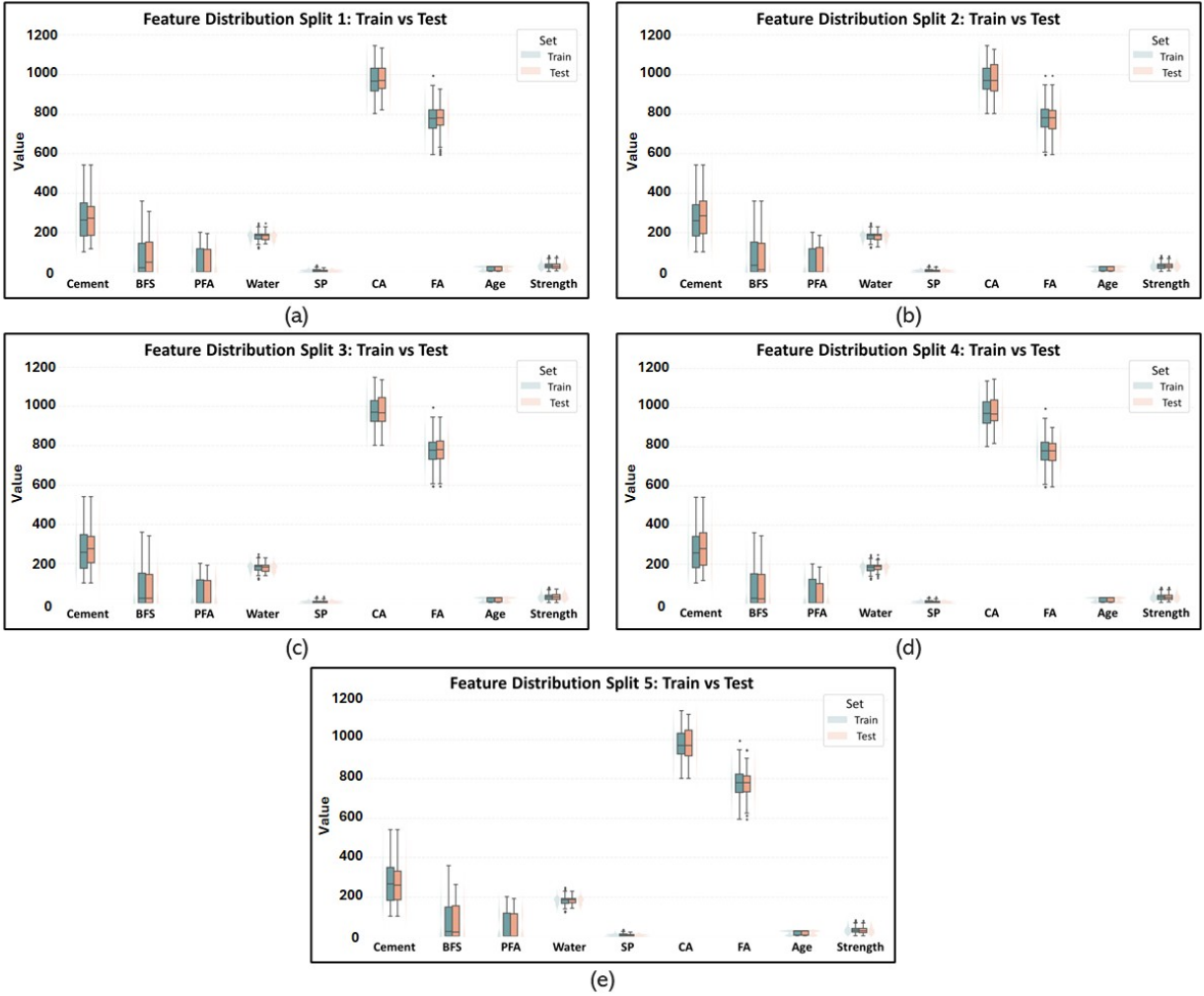


Figure 3: Data distribution of the five-split experiment setup (original scale).

### 3.3 Model Training and Inference Procedure

During training, the CoNN framework jointly optimizes the surrogate and imputation models using the cooperative objective defined in Eq. 5. The surrogate model learns to predict compressive strength from complete mix designs, while

the imputation model reconstructs masked inputs based on known variables and the performance feedback provided by the surrogate.

In the inference phase, the trained model receives partial mix specifications, where some variables are fixed by the user or by engineering constraints and others are left unspecified. A binary mask matrix encodes which variables are known (1) and which must be inferred (0). The masked design, along with the desired target strength, is passed through the imputation model to generate candidate values for the missing variables.

To simulate this scenario during evaluation, the test data were deliberately corrupted by masking a subset of variables according to predefined ratios, thereby simulating practical design constraints. To assess model robustness under varying levels of design incompleteness, partial inverse design scenarios were created by randomly masking up to five input variables per sample. Increasing the maximum number of masked variables progressively increased the difficulty of inference. All other experimental conditions, including network architecture, training hyperparameters, and the positions of masked variables were held constant across all experiments to ensure fair comparison. Because the imputation model explicitly receives the mask matrix as part of its input, it helps as a hint which variables are fixed and which are missing. This design enables the framework to adapt to different constraint scenarios without retraining, allowing multiple partial design configurations to be inferred simply by changing the mask input in a single forward pass. The overall inference process is illustrated in Fig. 4.

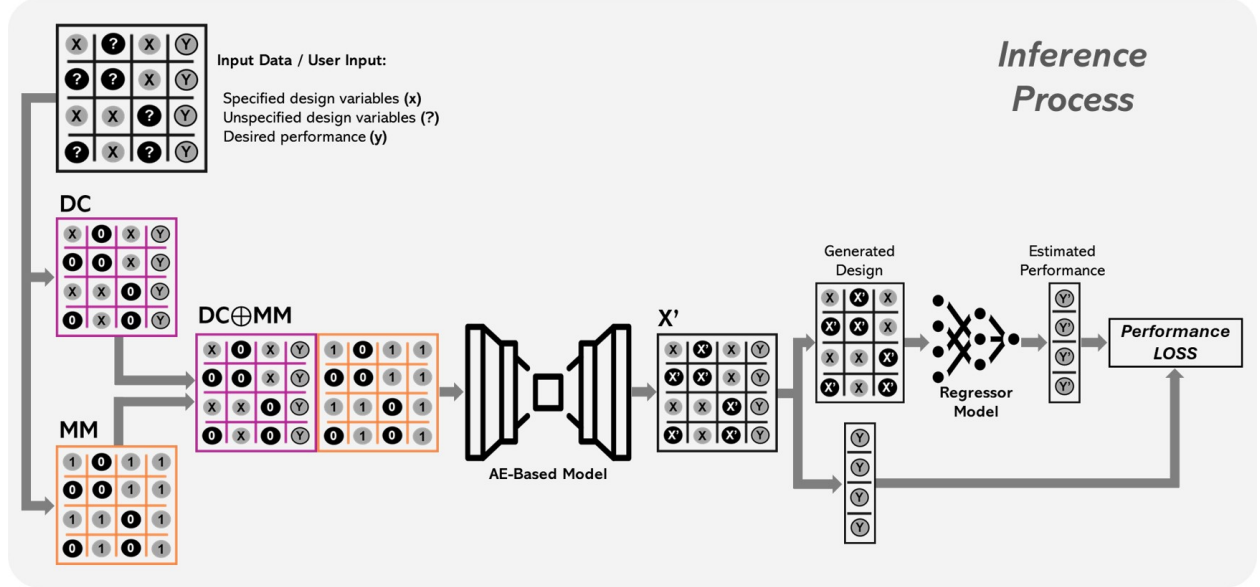


Figure 4: Inference process of Cooperative Neural Network (CoNN) (adopted from [26]).

### 3.4 Evaluation Objectives

Model performance was evaluated with two complementary objectives, prediction accuracy and computational efficiency. Prediction accuracy is defined as how closely the predicted performance of generated designs matched the target performance (compressive strength). For this, we measure the coefficient of determination ( $R^2$ ), mean absolute error (MAE), and mean squared error (MSE), averaged over the five evaluations. Their definitions are summarized in Table 2. Meanwhile, in contrast, computational efficiency is evaluated based on inference time, which reflects how quickly the model can produce results.

### 3.5 Comparative Methods

To rigorously evaluate the CoNN framework, we compared it with two representative paradigms for inverse design of HPC. First is the standalone autoencoder variants, and second is the Bayesian inference method based on GP regression. These baselines were chosen to distinguish the effects of the cooperative learning mechanism from those of probabilistic search-based inference, providing a balanced comparison between modern neural and classical Bayesian methodologies.

Table 2: Prediction accuracy metrics.

Metrics	Definition
Coefficient of Determination ( $R^2$ )	$1 - \frac{\sum_{i=1}^m (y_i - \hat{y}_i)^2}{\sum_{i=1}^m (y_i - \bar{y})^2}$
Mean Absolute Error (MAE)	$\frac{1}{m} \sum_{i=1}^m  y_i - \hat{y}_i $
Mean Squared Error (MSE)	$\frac{1}{m} \sum_{i=1}^m (y_i - \hat{y}_i)^2$

### 3.5.1 Standalone Autoencoder

The first baseline group corresponds to the CoNN architecture trained without cooperative feedback between the surrogate and imputation models. This includes three configurations which are the Denoising Autoencoder (DAE), Denoising Variational Autoencoder (DVAE), and Denoising Wasserstein Autoencoder (DWAE). These methods utilize the same network backbones and training hyperparameters as the full CoNN but omit (i) the mask matrix (MM), (ii) feature clipping, and (ii) the dual loss coupling with the surrogate model, as these components constitute key contributions of the proposed framework. Each variant isolates a specific modeling aspect:

- **DAE** serves as a deterministic reconstruction model trained only with a reconstruction loss to recover masked mix variables.
- **DVAE** extends this formulation by introducing a probabilistic latent space regularized by a Kullback–Leibler (KL) divergence term, allowing the generation of multiple feasible mix designs for the same input context.
- **DWAE** replaces the KL regularizer with a Maximum Mean Discrepancy (MMD) penalty, promoting smoother latent distributions and better generalization under limited data conditions.

By comparing these non-cooperative variants to the fully cooperative CoNN, we can directly assess how much performance improvement arises from the feedback interaction between the surrogate (performance evaluator) and the imputation model (design generator). All models were trained and tested on identical data partitions with the same optimization settings to ensure fair comparison.

### 3.5.2 Bayesian Inference with Gaussian Process Surrogate

The second baseline is based on the Bayesian inference framework originally proposed by Ke and Duan [1] for the full inverse design of HPC. Although their approach was not specifically developed for partial inverse design, it provides a probabilistic formulation that can be naturally extended to cases where only part of the input composition is unknown. The method combines a GP surrogate model with MCMC sampling via the MH algorithm, enabling probabilistic inference of mix designs consistent with a target property.

In the context of partial inverse design, the design variable vector  $\mathbf{X}$  can be partitioned into two subsets,  $\mathbf{X} = [\mathbf{X}_f, \mathbf{X}_u]$ , where  $\mathbf{X}_f$  represents the fixed (specified) variables and  $\mathbf{X}_u$  denotes the unknown variables to be inferred. The inverse problem can then be expressed in Bayesian form as:

$$p(\mathbf{X}_u | y^*, \mathbf{X}_f) \propto p(y^* | \mathbf{X}_u, \mathbf{X}_f) \cdot p(\mathbf{X}_u) \quad (6)$$

here,  $p(y^* | \mathbf{X}_u, \mathbf{X}_f)$  is the likelihood modeled by the GP surrogate, and  $p(\mathbf{X}_u)$  represents the prior distribution of the unknown variables. The posterior distribution  $p(\mathbf{X}_u | y^*, \mathbf{X}_f)$  quantifies the set of feasible mix designs that satisfy the target property under the given fixed-variable constraints. The likelihood term from the GP surrogate is typically modeled as a Gaussian distribution:

$$p(y^* | \mathbf{X}_u, \mathbf{X}_f) = \mathcal{N}(f(\mathbf{X}_u, \mathbf{X}_f), \sigma^2(\mathbf{X}_u, \mathbf{X}_f)) \quad (7)$$

where  $f(\mathbf{X}_u, \mathbf{X}_f)$  is the GP-predicted mean compressive strength, and  $\sigma^2(\mathbf{X}_u, \mathbf{X}_f)$  is the predictive variance.

The MCMC sampling procedure explores this posterior distribution to identify candidate compositions. For fair comparison with the proposed CoNN, the Bayesian-GP method was reimplemented under identical data partitions

and constraint settings. During inference, sampling was performed with search budgets of 1, 100, 1,000, 10,000, and 100,000 iterations, discarding the first 200 as burn-in to ensure convergence. The final mix design for each test case was computed as the mean of the post burn-in samples. While this Bayesian approach can produce statistically valid and uncertainty-aware designs, it requires extensive iterative sampling. In contrast, the proposed CoNN generates comparable or superior results in a single forward pass, achieving higher computational efficiency and practical usability for partial inverse design.

## 4 Results and Discussion

### 4.1 Comparison with Standalone Models

In our first quantitative comparison, we analyze the generated design candidates of the CoNN framework against standalone models, including DAE, DVAE, and DWAE, as explained in Section 3. The results are shown in Figs. 5, 7, and 8.

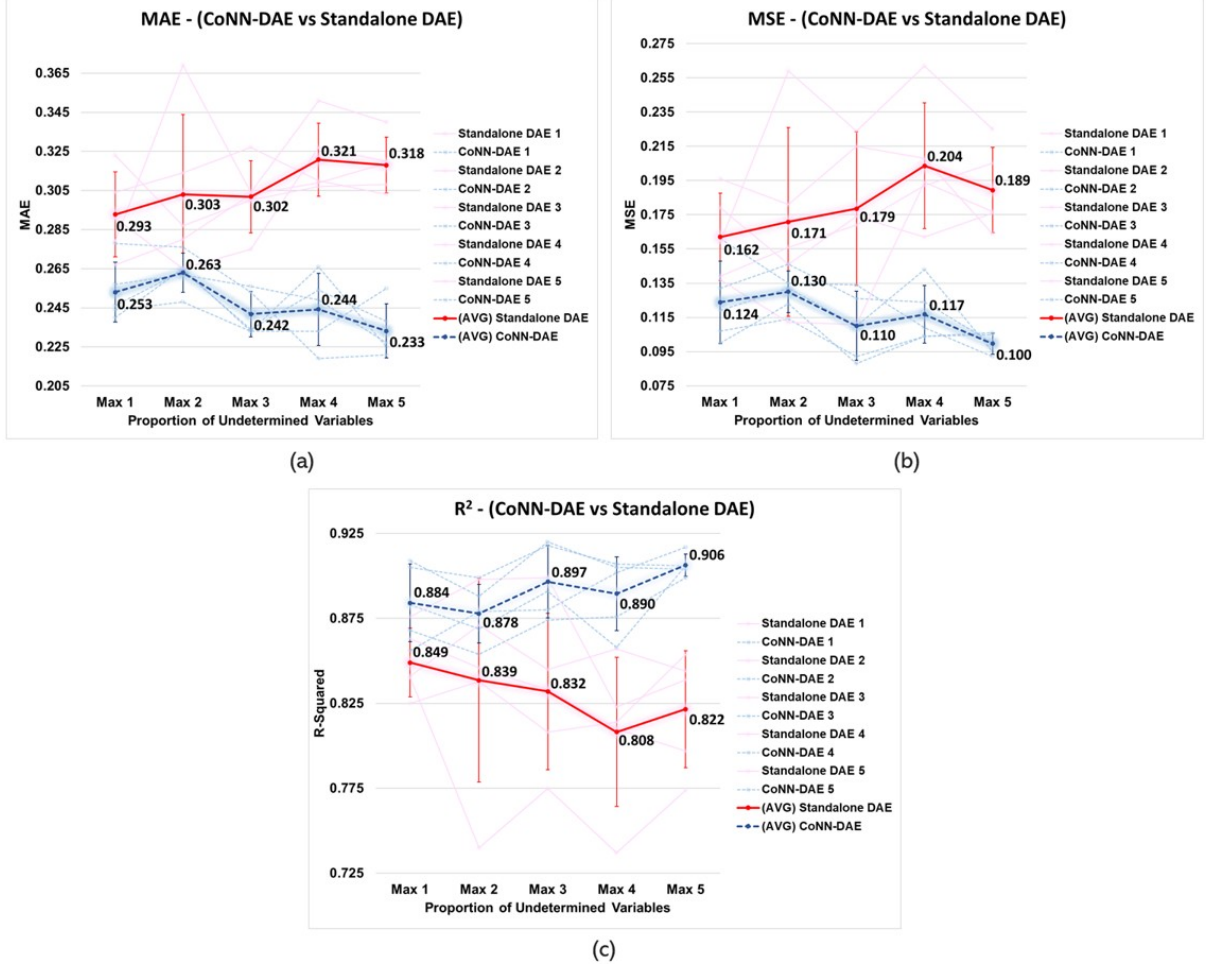


Figure 5: Performance comparison of standalone DAE and CoNN-DAE for (a) MAE, (b) MSE, and (c)  $R^2$  across varying proportions of undetermined variables. Average results over five runs ( $n = 5$ ) are shown with  $\pm 1$  standard deviation.

First, we evaluate the performance of the CoNN-DAE against the standalone DAE, as shown in Fig. 5. The results demonstrate that the CoNN framework consistently outperforms its standalone counterpart. Aggregated across five independent splits, the CoNN-DAE delivers more stable results with lower variance, whereas the standalone DAE exhibits instability. This creates a significant performance gap, particularly as the number of undetermined variables increase, the CoNN-DAE remains stable while the standalone DAE degrades. Specifically, the CoNN-DAE achieves

higher and more stable  $R^2$  values in the range of 0.878-0.906, compared to the standalone DAE, which declines from 0.849 to 0.822. The error metrics also highlight this advantage. The CoNN-DAE maintains lower MAE between 0.233-0.263, compared to 0.293-0.321 for the standalone DAE, and lower MSE between 0.100-0.130, whereas the standalone DAE shows an increasing trend from 0.162 to 0.189. Under the most challenging scenario with maximum five undetermined variables, the CoNN-DAE reduces MAE by 26.7% (from 0.318 to 0.233) and MSE by 47.0% (from 0.189 to 0.100), demonstrating its robustness in partial inverse design tasks, with the detailed comparison and statistical distributions shown in Fig. 6.

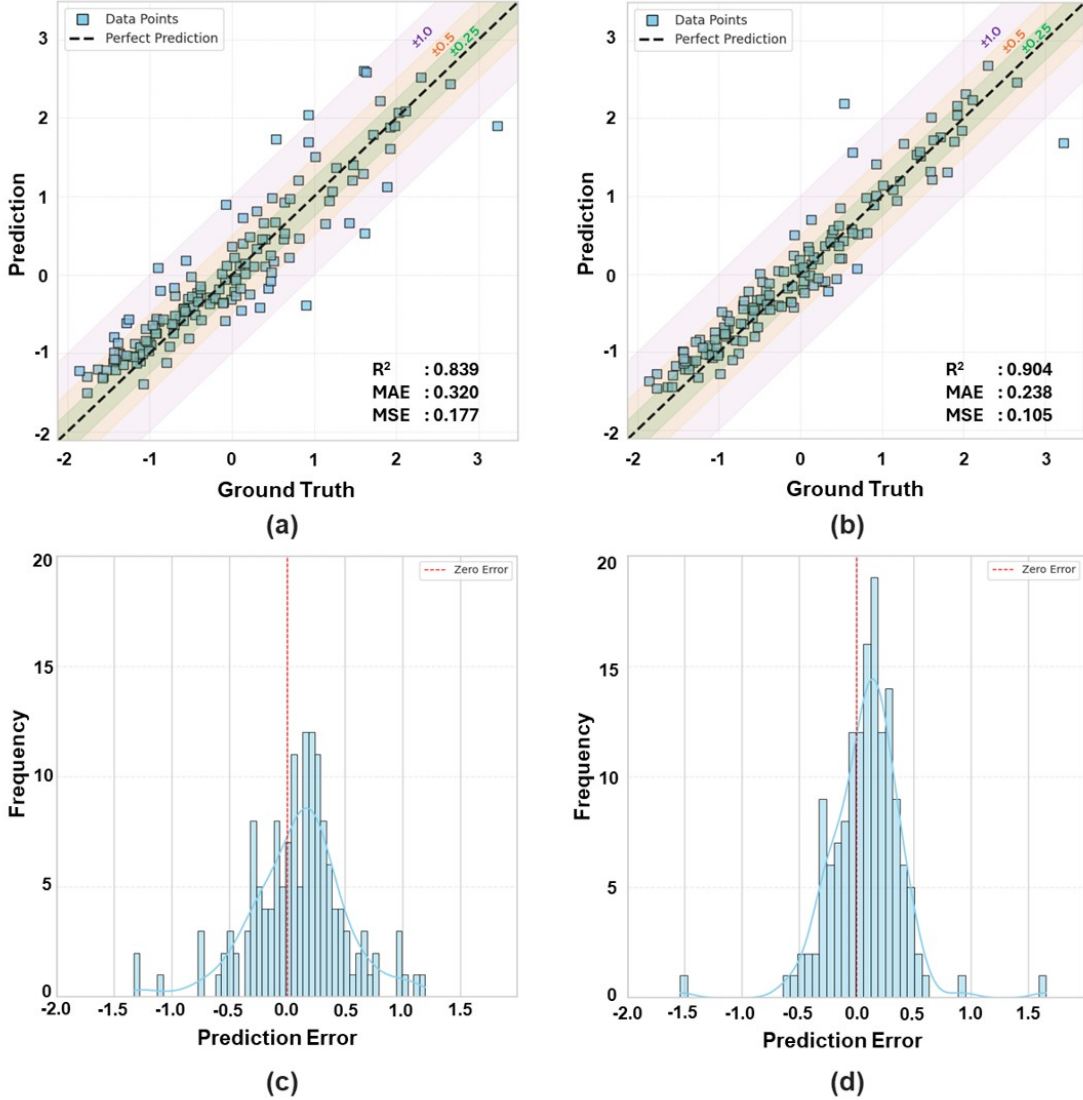


Figure 6: Comparative Results of Standalone DAE: (a) Prediction Result, (c) Error Ratio Histogram, and CoNN-DAE: (b) Prediction Result, (d) Error Ratio Histogram. Both on a maximum of 5 undetermined variables.

Next, we compare the CoNN-DVAE with the standalone DVAE, as shown in Fig. 7. The results clearly indicate that the CoNN framework substantially improves both accuracy and stability. The CoNN-DVAE achieves consistently higher  $R^2$  values, in the range 0.867-0.889, while the standalone DVAE declines from 0.840 to 0.780 as the number of undetermined variables increases. Similarly, the CoNN-DVAE maintains lower MAE values in the range 0.253-0.276, compared to 0.301-0.363 for the standalone DVAE. The advantage is even more evident in MSE, where the CoNN-DVAE remains stable at 0.120-0.141, while the standalone DVAE increases from 0.173 to 0.233. Under the most challenging condition with maximum five undetermined variables, the CoNN-DVAE reduces MAE by 24.0% (from 0.350 to 0.266) and MSE by 46.8% (from 0.233 to 0.124).

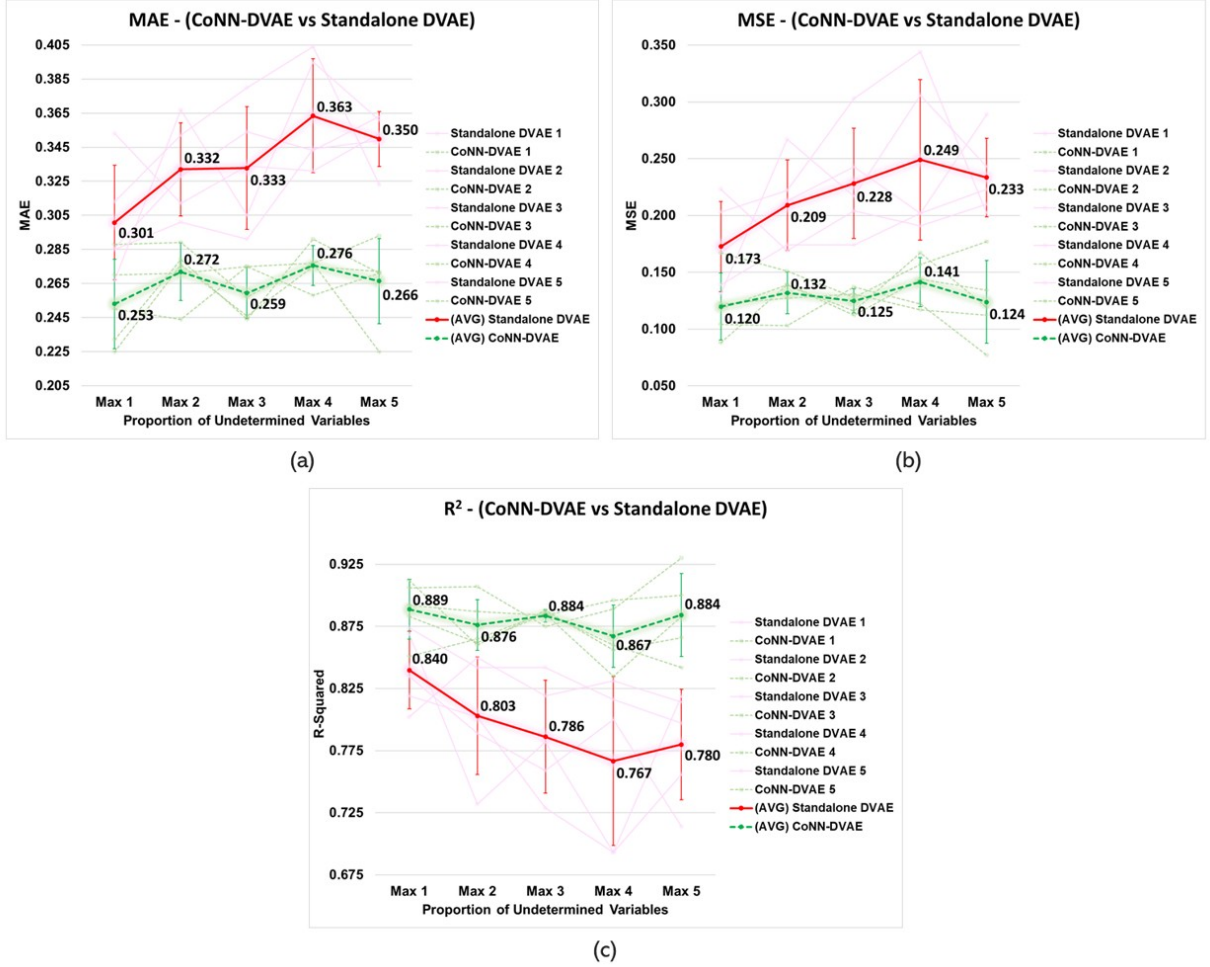


Figure 7: Performance comparison of standalone DVAE and CoNN-DVAE for (a) MAE, (b) MSE, and (c)  $R^2$  across varying proportions of undetermined variables. Average results over five runs ( $n = 5$ ) are shown with  $\pm 1$  standard deviation.

Finally, we compare the CoNN-DWAE with the standalone DWAE, as shown in Fig. 8. Similar to the previous cases, the CoNN framework consistently demonstrates superior performance and robustness. The CoNN-DWAE achieves stable  $R^2$  values in the range 0.881-0.916, while the standalone DWAE declines from 0.847 to 0.812 as the number of undetermined variables increases. In terms of error metrics, the CoNN-DWAE maintains lower MAE in the range 0.219-0.255, compared to 0.290-0.324 for the standalone DWAE. Likewise, the CoNN-DWAE achieves lower MSE in the range 0.089-0.126, whereas the standalone DWAE shows a rise in prediction error from 0.164 to 0.200. Under the most challenging scenario with maximum five undetermined variables, the CoNN-DWAE reduces MAE by 32.4% (from 0.324 to 0.219) and MSE by 55.5% (from 0.200 to 0.089).

Across all experiments, a consistent pattern is observed. Models within the CoNN framework are more robust and exhibit lower variance compared to their standalone counterparts, which are highly unstable and prone to large fluctuations. This difference is also evident across the five independent data splits, where CoNN models consistently yield tightly grouped results, while the standalone models show large variations from split to split, indicating instability and sensitivity to data partitioning. As task difficulty increases with a greater number of undetermined variables, the CoNN models remain stable, while standalone models suffer from declining performance and increasing error rates. This stability and reduced variance are particularly important in concrete research, where reliable and reproducible predictions are critical for guiding concrete mix design under practical constraints. Furthermore, the different CoNN variants serve complementary roles. The non-generative CoNN-DAE is well-suited for one-to-one mapping tasks such as reproducing high-performance concrete mix designs, while the generative CoNN-DVAE and CoNN-DWAE are more appropriate for one-to-many mapping tasks, enabling broader exploration of the feasible design space.

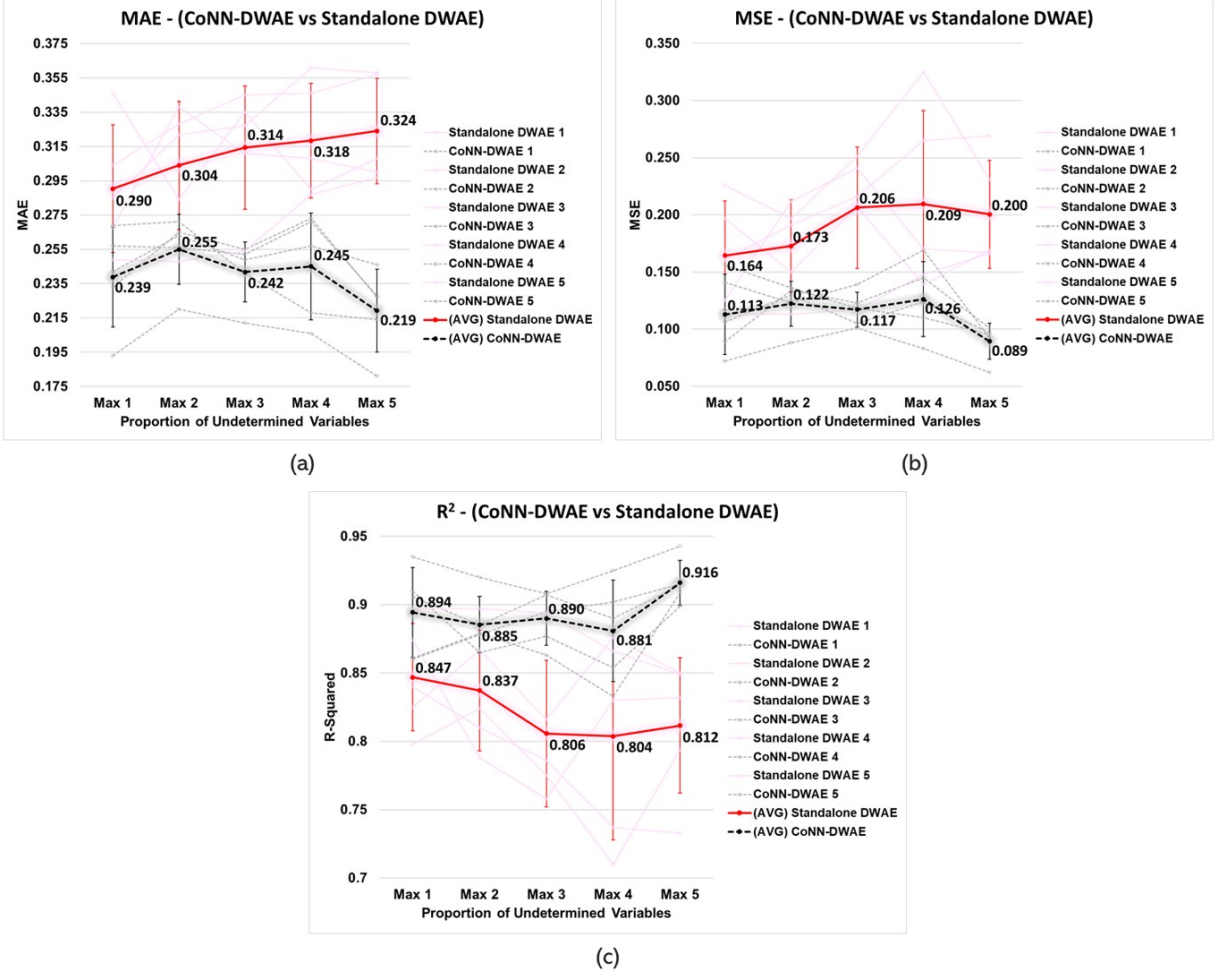


Figure 8: Performance comparison of standalone DWAE and CoNN-DWAE for (a) MAE, (b) MSE, and (c)  $R^2$  across varying proportions of undetermined variables. Average results over five runs ( $n = 5$ ) are shown with  $\pm 1$  standard deviation.

## 4.2 Comparison with Bayesian Inference

In this section, we compare the CoNN framework, including CoNN-DAE, CoNN-DVAE, and CoNN-DWAE, against Bayesian inference with a GP surrogate. As Bayesian inference is a well-established baseline for inverse design, especially in concrete research, this evaluation highlights the advantages of the proposed approach. Both predictive accuracy and computational efficiency are assessed in the following subsections.

### 4.2.1 Prediction Accuracy

We first compare the  $R^2$  performance of the CoNN framework against Bayesian inference with a GP surrogate, as shown in Fig. 9. Across all three variants, CoNN-DAE, CoNN-DVAE, and CoNN-DWAE consistently achieve higher and more stable  $R^2$  values than Bayesian inference. The CoNN models maintain higher and stable  $R^2$  values around 0.867-0.916 across different levels of undetermined variables, showing only minor fluctuations. In contrast, Bayesian inference begins with lower  $R^2$  value of 0.826 and deteriorates sharply as the number of undetermined variables increases, reaching as low as 0.675 at the most difficult setting. Under this condition, the CoNN framework demonstrates a relative improvement of approximately 33.3% in  $R^2$  compared to Bayesian inference, underscoring its superior predictive accuracy and robustness under high design uncertainty.

The error-based evaluation further emphasizes the superiority of the CoNN framework over Bayesian inference, as shown in Figs. 10 and 11. For MAE, all CoNN models maintain consistently low and stable errors across different

levels of undetermined variables, with values ranging from 0.219 to 0.276 and showing only minimal fluctuations for each model. In contrast, Bayesian inference exhibits steadily increasing errors, beginning with a MAE of 0.289 at the easiest setting and rising to 0.414 at the most difficult setting. A similar pattern is observed in the MSE results. The CoNN models sustain lower error values, ranging from 0.089 to 0.141, while Bayesian inference increases from 0.186 to 0.347 as task difficulty grows. At the most challenging level, the CoNN framework achieves substantial relative improvements, reducing MAE by approximately 42.2% and MSE by about 70%. These results confirm that the CoNN models not only deliver significantly lower error rates but also preserve remarkable stability as the number of undetermined variables increases, whereas Bayesian inference consistently deteriorates with higher task difficulty.

Taken together, the  $R^2$  and error-based evaluations clearly demonstrate the superiority of the CoNN framework over Bayesian inference. Across all scenarios, the CoNN models remain stable with low variance, while Bayesian inference shows a consistent decline in predictive accuracy and a steady increase in error as task difficulty grows. Moreover, Bayesian inference produces highly inconsistent outcomes across the five independent splits, with large fluctuations between runs despite using the same experimental setup. This instability underscores its sensitivity to data partitioning and highlights the difficulty of obtaining reliable results with sampling-based approaches. Such stability is particularly important in concrete research, where reproducible and reliable predictions are essential for guiding practical mix designs under uncertainty. By combining accurate forward prediction with robust handling of incomplete design information, the CoNN framework establishes itself as a more effective and dependable approach than Bayesian inference for partial inverse design tasks.

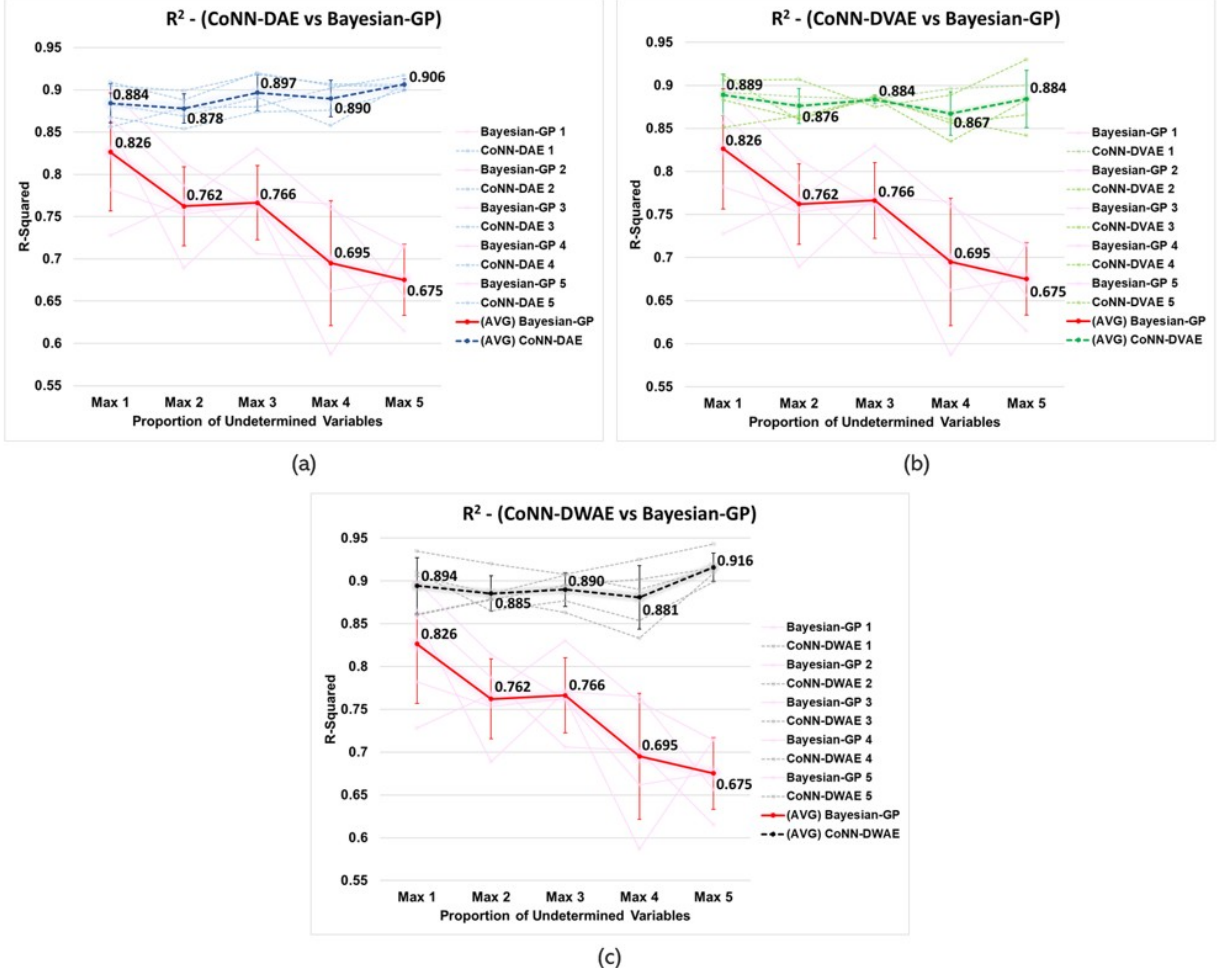


Figure 9: Comparative  $R^2$  performance of Bayesian-GP (100,000 MH searches) with (a) CoNN-DAE, (b) CoNN-DVAE, and (c) CoNN-DWAE across varying proportions of undetermined variables. Average results over five runs ( $n = 5$ ) are shown with  $\pm 1$  standard deviation.

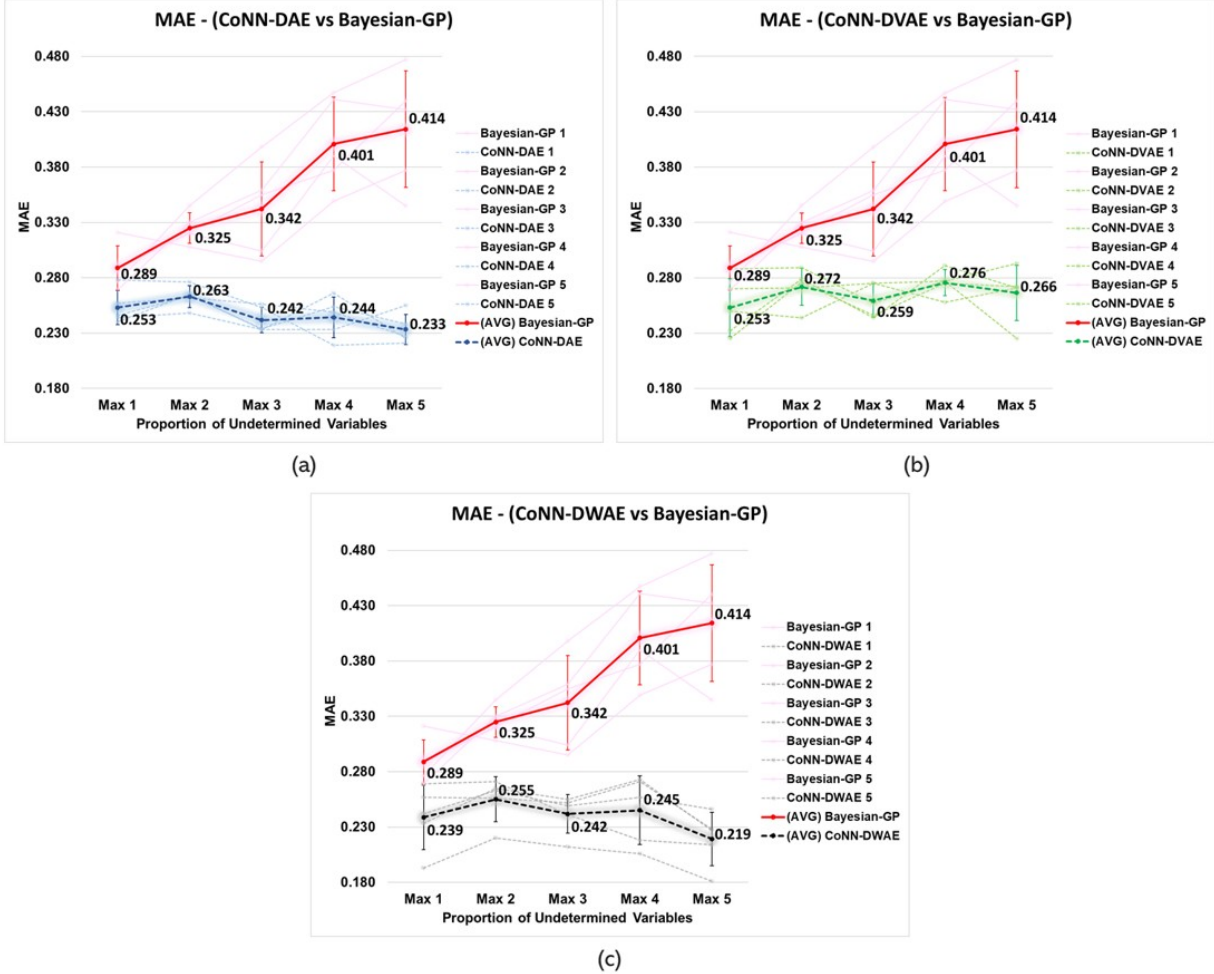


Figure 10: Comparative MAE performance of Bayesian-GP (100,000 MH searches) with (a) CoNN-DAE, (b) CoNN-DVAE, and (c) CoNN-DWAE across varying proportions of undetermined variables. Average results over five runs ( $n = 5$ ) are shown with  $\pm 1$  standard deviation.

#### 4.2.2 Computational Efficiency

In addition to predictive performance, computational efficiency was evaluated to assess the practicality of the inverse design frameworks. Fig. 12 illustrates the trade-off between inference time and performance ( $R^2$ ) for CoNN-DAE and Bayesian inference with a GP surrogate. The difference between the two approaches is striking. Bayesian inference relies on iterative MH searches, where accuracy gradually improves as the number of searches increases. However, this comes at the cost of rapidly escalating computational time. Even with 100,000 MH searches, which require considerable resources, Bayesian inference achieves lower  $R^2$  scores than the CoNN-DAE. In contrast, the CoNN-DAE delivers higher predictive accuracy with a single forward pass, completing the entire process in around one second. This comparison highlights the dual advantage of the CoNN framework: it not only achieves superior performance but also eliminates the inefficiencies inherent in iterative search-based methods.

Quantitatively, the efficiency gap is substantial. CoNN-DAE is approximately 16 $\times$  faster than Bayesian inference with just 1 MH search and nearly 7,333 $\times$  faster compared to 100,000 MH searches. Moreover, while Bayesian inference still underperforms at its most computationally expensive setting, the CoNN-DAE achieves an  $R^2$  that is about 34% higher. These results emphasize that the CoNN framework combines accuracy with efficiency in a way that Bayesian methods cannot match. Such capability is especially critical for practical applications in concrete research and engineering practice, where real-time or large-scale mix design exploration is often required under strict time constraints. By ensuring both robustness and speed, the CoNN model provides a scalable solution that makes partial inverse design feasible for deployment in real-world scenarios.

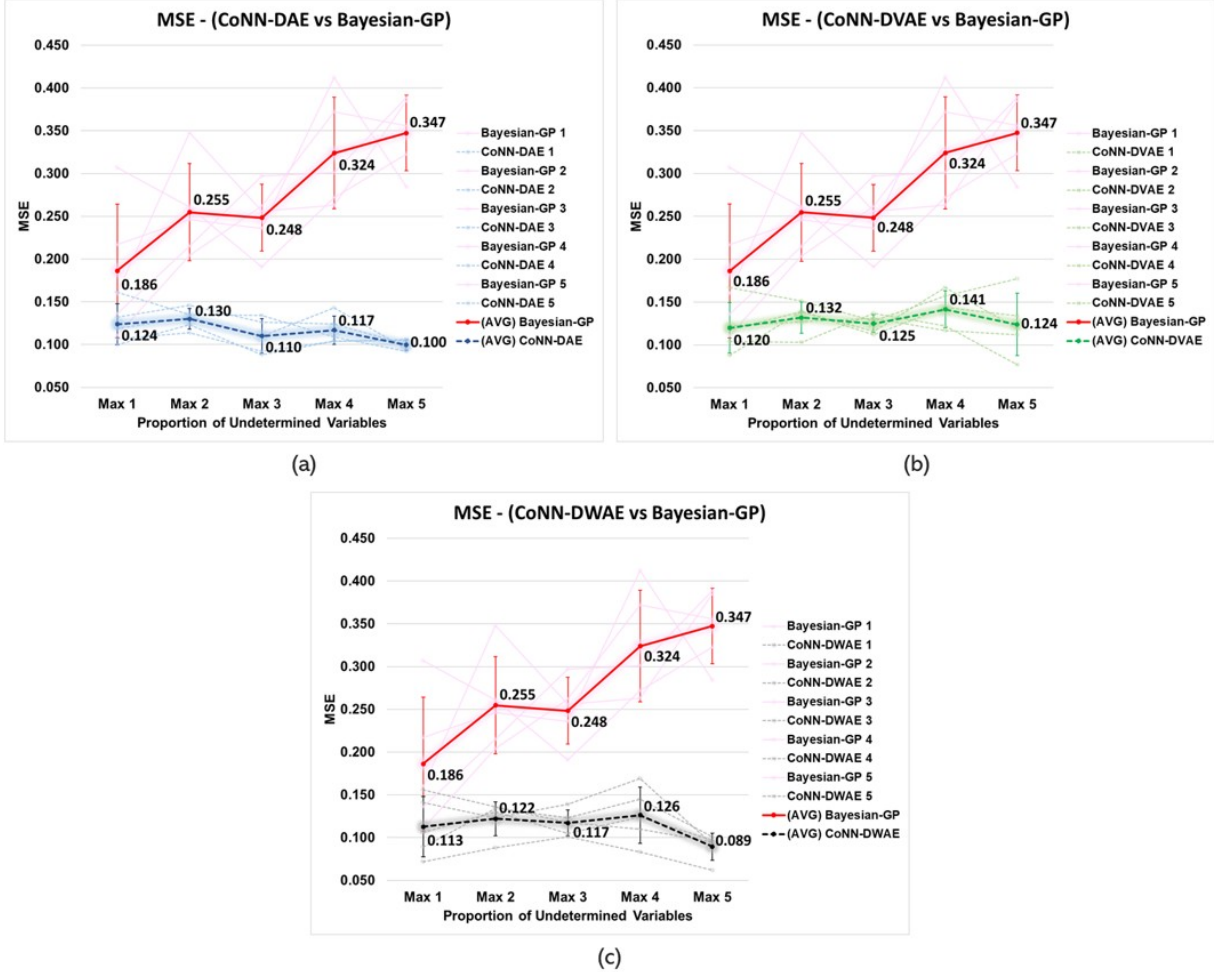


Figure 11: Comparative MSE performance of Bayesian-GP (100,000 MH searches) with (a) CoNN-DAE, (b) CoNN-DVAE, and (c) CoNN-DWAE across varying proportions of undetermined variables. Average results over five runs ( $n = 5$ ) are shown with  $\pm 1$  standard deviation.

#### 4.3 Perspective on Model Application

To demonstrate the applicability of the proposed framework in practical scenarios, Table 3 presents an example of generating an HPC mix design while meeting performance requirements under controlled design variables. In this case, a sample from the test set is used where the undetermined variables are cement, fly ash, and coarse aggregate, while all other variables are predetermined. The objective is to achieve the target compressive strength of 55.5 MPa. Although this example focuses specifically on cement, fly ash, and coarse aggregate, the framework is inherently flexible and can be applied to different subsets of variables without retraining, enabling random or scenario-specific selections depending on design requirements, as outlined in the previous section.

The results clearly highlight the superiority of the CoNN framework. CoNN models achieved the lowest deviations between the predicted and target strengths, with differences of +6.23 MPa, +4.22 MPa, and +5.41 MPa for CoNN-DAE, CoNN-DVAE, and CoNN-DWAE, respectively. By contrast, the standalone models and Bayesian-GP showed considerably larger deviations, ranging from +14.31 MPa to +16.44 MPa. These outcomes confirm that the CoNN framework not only generates feasible mix designs but also more reliably fulfills the target strength criteria provided by the user.

From the HPC perspective, result from the CoNN models are superior not only because they achieve strengths closer to the target, which is essential for ensuring long-term durability in practical applications, but also because they promote more economical and environmentally responsible designs. Unlike the standalone and Bayesian models,

which overshoot the target and waste cement due to their inability to impute the mix design correctly, the CoNN models consistently generate mix designs with reduced cement content. Since cement is both the most costly and the most carbon-intensive component of concrete, this reduction contributes to improve resource efficiency, potential cost savings, and substantial decreases in CO<sub>2</sub> emissions [38, 39]. While these benefits may vary depending on inference conditions, the results clearly demonstrate the importance of developing models capable of imputing undetermined variables accurately while fulfilling the required design criteria.

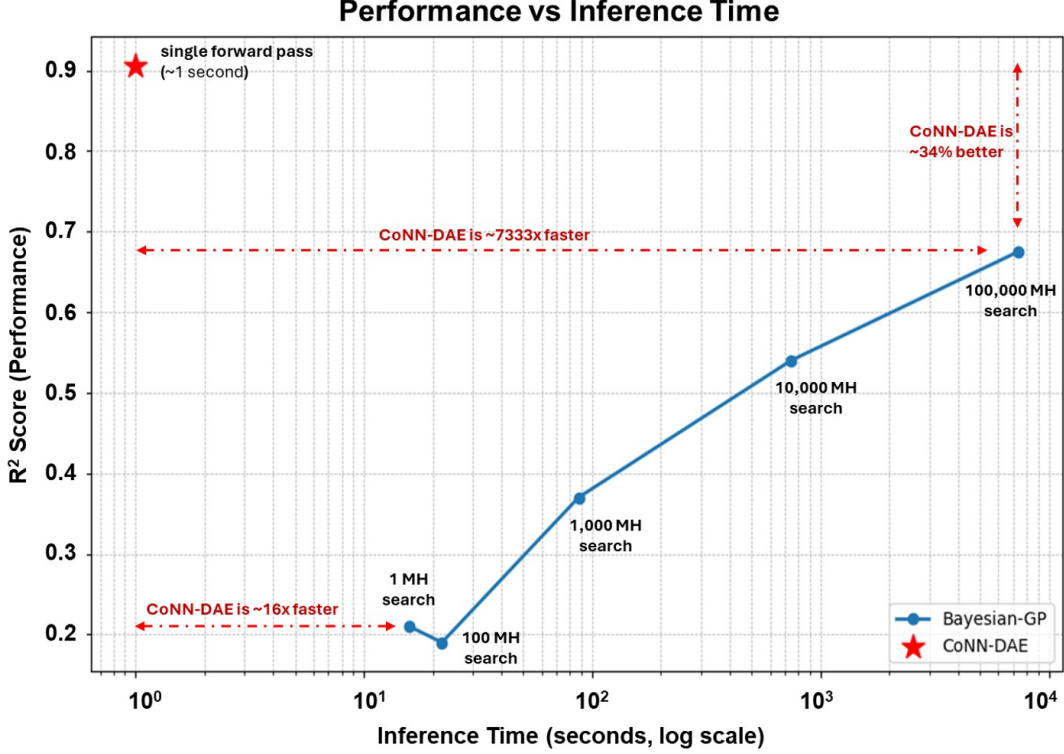


Figure 12: Comparison of computational efficiency and predictive performance ( $R^2$ ) between CoNN-DAE and Bayesian inference under settings with up to five undetermined variables for the all-test data.

Table 3: Application and comparison of generated design results from all models.

Category	Model	Design variables								Estimation strength (diff)
		Cement	BFS	PFA	Water	SP	CA	FA	Age	
User input	-	...	212.50	...	155.70	14.30	...	880.40	28.00	<b>55.50</b>
Modelling results	Bayesian-GP	<b>372.54</b>	212.50	<b>89.56</b>	155.70	14.30	<b>943.51</b>	880.40	28.00	<b>69.81 (+14.31)</b>
	Standalone DAE	<b>381.83</b>	212.50	<b>20.12</b>	155.70	14.30	<b>957.71</b>	880.40	28.00	<b>70.67 (+15.18)</b>
	Standalone DVAE	<b>377.34</b>	212.50	<b>35.61</b>	155.70	14.30	<b>915.17</b>	880.40	28.00	<b>71.67 (+16.18)</b>
	Standalone DWAE	<b>429.14</b>	212.50	<b>2.97</b>	155.70	14.30	<b>828.02</b>	880.40	28.00	<b>71.94 (+16.44)</b>
	Cooperative DAE	<b>294.17</b>	212.50	<b>44.94</b>	155.70	14.30	<b>971.42</b>	880.40	28.00	<b>61.72 (+6.23)</b>
	Cooperative DVAE	<b>265.80</b>	212.50	<b>65.40</b>	155.70	14.30	<b>961.96</b>	880.40	28.00	<b>59.72 (+4.22)</b>
	Cooperative DWAE	<b>283.38</b>	212.50	<b>88.24</b>	155.70	14.30	<b>951.90</b>	880.40	28.00	<b>60.91 (+5.41)</b>

## 5 Conclusion

This study applied a Cooperative Neural Networks (CoNN) framework to address the challenge of partial inverse design in the cement and concrete domain, marking its first application to HPC. Unlike conventional forward or inverse design approaches, partial inverse design allows only a subset of variables to remain undetermined while others are fixed by design constraints. The framework, composed of an imputation model and a surrogate model trained under cooperative learning, enables the generation of mix designs under flexible constraints with a single forward pass.

The experimental results demonstrate several key contributions. First, the CoNN framework consistently outperformed standalone autoencoder variants (DAE, DVAE, and DWAE), achieving higher predictive accuracy, lower error rates, and substantially reduced variance as the number of undetermined variables increased. This robustness is particularly valuable in practical scenarios, where stable and reproducible results are critical despite rising task complexity. Second, when benchmarked against Bayesian inference with GP surrogates, the CoNN models not only achieved superior accuracy but also demonstrated remarkable computational efficiency, producing valid mix designs within a single forward pass. This efficiency stands in sharp contrast to Bayesian approaches that require thousands of iterative searches, further underscoring the practicality and scalability of the CoNN framework for inverse design in concrete research.

Despite these promising results, several limitations remain. The dataset used in this study is relatively scarce, which may limit the generalizability of the findings compared to scenarios where larger and more diverse datasets are available. Additionally, while the framework shows potential to provide economic and environmental benefits in concrete research, the extent of these advantages may vary depending on inference conditions and design scenarios. Future work could address these challenges by incorporating larger-scale and more diverse datasets to strengthen training, as well as exploring more advanced strategies such as neural networks that capture physics information, which enable domain knowledge to be injected into the learning process through common-sense or policy-driven shape constraints, thereby better capturing the physical and mechanistic relationships governing HPC mix design.

In summary, this research pioneers the application of CoNN for partial inverse design in HPC, demonstrating strong predictive accuracy, computational efficiency, and potential sustainability benefits. With further refinements in data availability and methodological integration, the framework has the potential to evolve into a powerful tool for intelligent, constraint-aware material design.

## Acknowledgements

This research was supported by the MSIT (Ministry of Science and ICT), Korea, under the ICAN (ICT Challenge and Advanced Network of HRD) support program supervised by the IITP (Institute for Information & Communications Technology Planning & Evaluation) (IITP-2025-RS-2023-00259806).

## References

- [1] Xinyuan Ke and Yu Duan. A bayesian machine learning approach for inverse prediction of high-performance concrete ingredients with targeted performance. *Construction and Building Materials*, 270:121424, 2021.
- [2] I.-C. Yeh. Modeling of strength of high-performance concrete using artificial neural networks. *Cement and Concrete Research*, 28(12):1797–1808, 1998.
- [3] P.C Aı̄tcin. The durability characteristics of high performance concrete: a review. *Cement and Concrete Composites*, 25(4):409–420, 2003.
- [4] M.H. Fazel Zarandi, I.B. Türksen, J. Sobhani, and A.A. Ramezanianpour. Fuzzy polynomial neural networks for approximation of the compressive strength of concrete. *Applied Soft Computing*, 8(1):488–498, 2008.
- [5] S. Wijesundara, K. Wijesundara, and S. Bandara. Machine learning approach for predicting the compressive strength of ultra-high performance fiber reinforced concrete (UHPFRC). *Structures*, 75:108704, 2025.
- [6] Adithya Challapalli, Dhrumil Patel, and Gouqiang Li. Inverse machine learning framework for optimizing lightweight metamaterials. *Materials & Design*, 208:109937, 2021.
- [7] Chathura Wanigasekara, Ebrahim Oromiehie, Akshya Swain, B. Gangadhara Prusty, and Sing Kiong Nguang. Machine learning-based inverse predictive model for AFP based thermoplastic composites. *Journal of Industrial Information Integration*, 22:100197, 2021.
- [8] Zuoxu Wang, Pai Zheng, Xinyu Li, and Chun-Hsien Chen. Implications of data-driven product design: From information age towards intelligence age. *Advanced Engineering Informatics*, 54:101793, 2022.

[9] Zhoumingju Jiang, Hui Wen, Fred Han, Yunlong Tang, and Yi Xiong. Data-driven generative design for mass customization: A case study. *Advanced Engineering Informatics*, 54:101786, 2022.

[10] Arash Ebrahimian, Hossein Mohammadi, and Nima Maftoon. Material characterization of human middle ear using machine-learning-based surrogate models. *Journal of the Mechanical Behavior of Biomedical Materials*, 153:106478, 2024.

[11] Zeyuan Miao, Lee Margetts, Anastasia N. Vasileiou, and Hujun Yin. Surrogate model development using simulation data to predict weld residual stress: A case study based on the NeT-TG1 benchmark. *International Journal of Pressure Vessels and Piping*, 206:105014, 2023.

[12] I-Cheng Yeh. Analysis of strength of concrete using design of experiments and neural networks. *Journal of Materials in Civil Engineering*, 18(4):597–604, 2006.

[13] Zhanzhao Li, Jinyoung Yoon, Rui Zhang, Farshad Rajabipour, Wil V. Srubar Iii, Ismaila Dabo, and Aleksandra Radlińska. Machine learning in concrete science: applications, challenges, and best practices. *npj Computational Materials*, 8(1):127, 2022.

[14] Jinjun Xu, Xinyu Zhao, Yong Yu, Tianyu Xie, Guosong Yang, and Jianyang Xue. Parametric sensitivity analysis and modelling of mechanical properties of normal- and high-strength recycled aggregate concrete using grey theory, multiple nonlinear regression and artificial neural networks. *Construction and Building Materials*, 211:479–491, 2019.

[15] B. Ouyang, Y. Li, F. Wu, H. Yu, Y. Wang, G. Sant, and M. Bauchy. Predicting concrete's strength by machine learning: Balance between accuracy and complexity of algorithms. *ACI Materials Journal*, 117(6), 2020.

[16] Hoang Nguyen, Thanh Vu, Thuc P. Vo, and Huu-Tai Thai. Efficient machine learning models for prediction of concrete strengths. *Construction and Building Materials*, 266:120950, 2021.

[17] Khandaker M. A. Hossain, Muhammed S. Anwar, and Shirin G. Samani. Regression and artificial neural network models for strength properties of engineered cementitious composites. *Neural Computing and Applications*, 29(9):631–645, 2018.

[18] Tuan Nguyen-Sy, Jad Wakim, Quy-Dong To, Minh-Ngoc Vu, The-Duong Nguyen, and Thoi-Trung Nguyen. Predicting the compressive strength of concrete from its compositions and age using the extreme gradient boosting method. *Construction and Building Materials*, 260:119757, 2020.

[19] Min-Yuan Cheng, Jui-Sheng Chou, Andreas F.V. Roy, and Yu-Wei Wu. High-performance concrete compressive strength prediction using time-weighted evolutionary fuzzy support vector machines inference model. *Automation in Construction*, 28:106–115, 2012.

[20] Mengxi Zhang, Mingchao Li, Yang Shen, Qiubing Ren, and Jinrui Zhang. Multiple mechanical properties prediction of hydraulic concrete in the form of combined damming by experimental data mining. *Construction and Building Materials*, 207:661–671, 2019.

[21] Junfei Zhang, Dong Li, and Yuhang Wang. Toward intelligent construction: Prediction of mechanical properties of manufactured-sand concrete using tree-based models. *Journal of Cleaner Production*, 258:120665, 2020.

[22] Tandré Oey, Scott Jones, Jeffrey W. Bullard, and Gaurav Sant. Machine learning can predict setting behavior and strength evolution of hydrating cement systems. *Journal of the American Ceramic Society*, 103(1):480–490, 2020.

[23] Afshin Marani and Moncef L. Nehdi. Machine learning prediction of compressive strength for phase change materials integrated cementitious composites. *Construction and Building Materials*, 265:120286, 2020.

[24] Jui-Sheng Chou and Chih-Fong Tsai. Concrete compressive strength analysis using a combined classification and regression technique. *Automation in Construction*, 24:52–60, 2012.

[25] Ishana M, Leherijah S, K. Vijai, Sivaranjani D, and Jessica Preethi B. Optimized ANN-GA model for predicting the compressive strength of high-performance concrete. In *2025 Fourth International Conference on Smart Technologies, Communication and Robotics (STCR)*, pages 1–6. IEEE, 2025.

[26] Agung Nugraha, Hyerin Kwon, Gyeongho Park, and Jihwan Lee. Cooperative neural networks for inverse design: Integrating denoising autoencoder and surrogate model for partial design variable imputation. *Engineering Applications of Artificial Intelligence*, 162:112453, 2025.

[27] Yimiao Huang, Junfei Zhang, Foo Tze Ann, and Guowei Ma. Intelligent mixture design of steel fibre reinforced concrete using a support vector regression and firefly algorithm based multi-objective optimization model. *Construction and Building Materials*, 260:120457, 2020.

[28] Junfei Zhang, Yimiao Huang, Farhad Aslani, Guowei Ma, and Brett Nener. A hybrid intelligent system for designing optimal proportions of recycled aggregate concrete. *Journal of Cleaner Production*, 273:122922, 2020.

[29] Khuong Le Nguyen, Minhaz Uddin, and Thong M. Pham. Generative artificial intelligence and optimisation framework for concrete mixture design with low cost and embodied carbon dioxide. *Construction and Building Materials*, 451:138836, 2024.

[30] Yi-Xin Zhang, Qiao Zhang, Ling-Yu Xu, Wei Hou, You-Shui Miao, Yang Liu, and Bo-Tao Huang. Transfer learning for intelligent design of lightweight strain-hardening ultra-high-performance concrete (SH-UHPC). *Automation in Construction*, 175:106241, 2025.

[31] Jie Yu, Yiwei Weng, Jiangtao Yu, Wenguang Chen, Shuainan Lu, and Kequan Yu. Generative AI for performance-based design of engineered cementitious composite. *Composites Part B: Engineering*, 266:110993, 2023.

[32] *Eurocode 2: design of concrete structures : part 1-1: general rules and rules for buildings*. British Standards Institution, 2004. OCLC: 71075024.

[33] Alexandre Mathern, Olof Skogby Steinholtz, Anders Sjöberg, Magnus Önnheim, Kristine Ek, Rasmus Rempling, Emil Gustavsson, and Mats Jirstrand. Multi-objective constrained bayesian optimization for structural design. *Structural and Multidisciplinary Optimization*, 63(2):689–701, 2021.

[34] Shengbo Wang and Ke Li. Constrained bayesian optimization under partial observations: Balanced improvements and provable convergence. *Proceedings of the AAAI Conference on Artificial Intelligence*, 38(14):15607–15615, 2024.

[35] Sasan Amini, Inneke Vannieuwenhuyse, and Alejandro Morales-Hernández. Constrained bayesian optimization: A review. *IEEE Access*, 13:1581–1593, 2025.

[36] Diederik P Kingma and Max Welling. Auto-encoding variational bayes, 2013. Version Number: 11.

[37] Ilya Tolstikhin, Olivier Bousquet, Sylvain Gelly, and Bernhard Schoelkopf. Wasserstein auto-encoders, 2019.

[38] Francisco Agrela, Manuel Rosales, Mónica López Alonso, Javier Ordóñez, and Gloria M. Cuenca-Moyano. Life-cycle assessment and environmental costs of cement-based materials manufactured with mixed recycled aggregate and biomass ash. *Materials*, 17(17):4357, 2024.

[39] Ardavan Yazdanbakhsh, Lawrence C. Bank, Thomas Baez, and Iddo Wernick. Comparative LCA of concrete with natural and recycled coarse aggregate in the new york city area. *The International Journal of Life Cycle Assessment*, 23(6):1163–1173, 2018.